

Detection of Breeding Blankets Using Antineutrinos

Bernadette K. Cogswell^a and Patrick Huber^b

^aProgram on Science and Global Security, Princeton University, Princeton, NJ, USA; ^bCenter for Neutrino Physics, Department of Physics, Virginia Polytechnic Institute and State University, Blacksburg, VA, USA

ABSTRACT

The Plutonium Management and Disposition Agreement between the United States and Russia makes arrangements for the disposal of 34 metric tons of excess weapon-grade plutonium. Under this agreement Russia plans to dispose of its excess stocks by processing the plutonium into fuel for fast breeder reactors. To meet the disposition requirements this fuel would be burned while the fast reactors are run as burners, i.e., without a natural uranium blanket that can be used to breed plutonium surrounding the core. This article discusses the potential application of antineutrino monitoring to the verification of the presence of a breeding blanket. It is found that a 36 kg antineutrino detector, exploiting coherent elastic neutrino-nucleus scattering and made of silicon could determine the presence of a breeding blanket at a liquid sodium cooled fast reactor at the 95 percent confidence level within 90 days.

ARTICLE HISTORY

Received 17 December 2015
Accepted 18 February 2016

Introduction

Under the Plutonium Management and Disposition Agreement (PMDA)¹ the United States and Russia each agreed to dispose of 34 metric tons worth of weapon-grade plutonium. Three disposition options have been considered. First, the excess plutonium could be immobilized in glass along with high level radioactive waste and buried. Second, the plutonium to be disposed of could be processed to make mixed oxide (MOX) fuel and burned in light water reactors. Third, the plutonium could be processed into fast reactor fuel and burned there. While the United States is pursuing the first two options, Russia remains committed to pursuing the third option. For both reactor-based methods, three factors contribute to the disposition goal: First, odd-mass plutonium isotopes are directly fissioned. Second, even-mass plutonium isotopes are produced via neutron capture on odd-mass plutonium isotopes. In combination, this leads to a significant reduction of the relative plutonium-239 content, making the material less weapon-usable. Third, the fission fragments in the spent fuel produce an intense radiation field, effectively increasing the difficulty,

CONTACT Patrick Huber  pahuber@vt.edu  Center for Neutrino Physics, Department of Physics (0435), Virginia Tech, Blacksburg, VA 24061, USA.

Color versions of one or more of the figures in the article can be found online at www.tandfonline.com/gsgs.

© 2016 Taylor & Francis Group, LLC

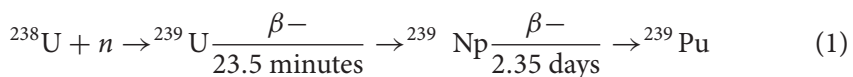
complexity, and time scale of a potential weapon application. All three aspects scale directly with the total fuel burn-up and, thus, current verification proposals focus on methods to ensure a certain minimum burn-up is achieved.

In the fast reactor scheme the excess weapon-grade plutonium would be blended down into fast reactor fuel that would be used in the Russian BN-600 and the Russian BN-800 reactors. Under this disposition method, Russia has agreed to run these two reactors as “burners” not “breeders.” This means that the fast reactors would be loaded with the fuel containing the weapon-grade plutonium to be disposed of, but, most likely, no blanket of natural uranium would be placed around the core, such that the reactor does not simultaneously breed new plutonium while burning excess plutonium. As part of a verification regime, such as one that could be overseen by the International Atomic Energy Agency (IAEA), technologies would be needed that could help monitor that a fast reactor is being run as a burner and not as a breeder.

External core monitoring methods exist, such as using power measurements and neutron and gamma flux measurements along with reactor design information to estimate the fissile material content in the core, e.g., uranium-235, plutonium-239, and plutonium-241, which would provide a means to verify proper reactor use. However, the radiation and heat signatures from a breeding blanket are relatively weak compared to the reactor core and, therefore, it is far from obvious that conventional techniques are able to conclusively test for the presence of a blanket once the reactor vessel has been closed. Furthermore, these methods use technologies that must be located within the facility and can therefore sometimes be considered intrusive by the party being inspected. Other options, like in-core monitoring, are even more intrusive and may be objected to by the party being inspected in cases where core access and design information are protected for proprietary reasons. Ideally, less intrusive technologies could be developed and deployed to help monitor reactor operations from outside the facility, such as antineutrino detectors.

Fast reactors

A fast reactor that produces more fissile material (which can be fissioned with neutrons of any energy) than it consumes as fuel is designated as a “breeder” reactor.² In the case of the current study, breeder reactors include a fertile blanket material (which can only be fissioned with low energy thermal neutrons) of natural or depleted uranium that is loaded around the sides (the radial blanket) and above and below (the axial blanket) the fast reactor core containing MOX fuel enriched in plutonium-239. Fission in the core generates a high neutron flux that bombards the blanket. Neutron capture on uranium-238 in the blanket produces plutonium-239 through a succession of two radioactive beta decays (β^-)



where the half-life of the isotopic decay is given in the denominators.

Since a breeder reactor is one that produces more fissile material than it consumes, it is of interest to seek non-intrusive verification technologies, i.e., technologies that do not need to be installed in the flow of plant operations, but can still be used to gather qualitatively meaningful information about the blanket. Therefore, monitoring at a distance in a non-intrusive manner requires a highly penetrating radiation. The most abundant radiation-producing reaction occurring in the breeding blanket during reactor operation is radioactive beta decay due to neutron capture (as shown in Eq. 1),



where P is the parent nuclei, D is the daughter nuclei, e^- is an electron, and $\bar{\nu}_e$ is an electron antineutrino. In this decay process (Eq. 2), a neutron within the nucleus decays into a proton, emitting an electron and an electron antineutrino in order to conserve energy and momentum. Between the electron and antineutrino emitted, the antineutrino is the best candidate particle for non-intrusive monitoring since it is weakly interacting (with a cross section of roughly 10^{-42} cm² it can pass through a light-year, about 9.5×10^{12} kilometers (km), worth of lead without significant attenuation) and abundantly produced (at a rate of roughly 10^{20} per second (s) from a 1 gigawatt thermal (GWt) reactor).

Since beta decay is a three-body decay, the antineutrinos produced, like the electrons, will have a range of emitted energies. Fission itself does not produce antineutrinos, this happens in the beta-decays of neutron-rich fission fragments. Approximately six antineutrinos are emitted per fission with about 99 percent of all antineutrinos emitted coming from the fission of four main isotopes, uranium-235, uranium-238, plutonium-239, and plutonium-241. These antineutrinos have an energy range up to 12 mega-electronvolts (MeV). In the remainder of this paper antineutrinos emitted by fission processes will be labelled FANs (fission antineutrinos). Neutron capture on uranium-238 results in two successive beta decays to plutonium-239, thus the neutron capture process produces two antineutrinos with energies up to about 1.26 MeV. Throughout the remainder of this paper the antineutrinos emitted by the capture process will be labelled CANs (capture antineutrinos). Observing FANs permits the estimation of a number of useful safeguards quantities of interest because of the underlying connection between antineutrino emission and core isotopics: the average number of antineutrinos emitted, their specific energy range, average energy, and peak energy all vary by isotope.³ Therefore, observing a reactor antineutrino spectrum permits a backward extraction of the core fission rates by isotope (of only the four main antineutrino producing isotopes already listed) and as a result an estimate of quantities such as the reactor power, the core fissile material content, and the age and burn up of the reactor fuel.

This opportunity for monitoring the core power and key fissile composition using antineutrino emissions was first recognized in 1977.⁴ A group conducted a demonstration experiment in 1984⁵ and again in 1994⁶ using a 0.5 ton liquid scintillator antineutrino detector deployed below a 1.375 GWt reactor core at the Rovno power plant in the Ukraine. With their small prototype they were able to show that

reactor antineutrinos could be successfully detected and be used to estimate the reactor power to within 3 percent of a temperature-based monitoring method as well as be used to estimate the total uranium-235, uranium-238, plutonium-239, and plutonium-241 isotopic content to within a few percent of a thermal method. A similar additional demonstration experiment to show that reactor antineutrino emissions could be used for safeguards purposes was conducted starting in 2003 using a 0.64 ton liquid scintillator device deployed below ground, this time operating successfully unattended for one year, near two 3.4 GWt reactor units at the San Onofre Generating Station in the United States.⁷ Recently, the Nucifer collaboration demonstrated a practical liquid scintillator detector operating very close to the reactor core and the surface.⁸ For a review of work in the area of antineutrino detection and safeguards, see for example A. Bernstein et al.⁹ Also, more recent theoretical investigations have focused on studying the applications of antineutrino detectors to the study of MOX fuels¹⁰ and converted light water reactors (LWRs)¹¹ (such as might be used for the disposition of excess U.S. weapons plutonium), the situation in Iran,¹² and a hypothetical scenario involving antineutrino detectors and the North Korean crisis of 1994.¹³

Unfortunately, for the purposes of monitoring a breeding blanket, much of the existing antineutrino detector technology cannot be used due to a confounding physics problem: the CAN signal energy is below the detection threshold for the existing technology. The technologies that have been used all rely on detecting antineutrinos using inverse beta decay (IBD), which is neutrino capture on a free proton,



where p is a proton and e^+ is a positron. This reaction has a threshold of $m_n - m_p + 2m_e = 1.8$ MeV. FANs are produced with energies up to 12 MeV so they can be detected using IBD. However, CANs have a maximum energy of 1.26 MeV, which is below the IBD threshold. Therefore, detecting CANs requires a novel antineutrino detection channel.

Coherent antineutrino detection

For low energy CANs a viable detection channel is coherent elastic neutrino nucleus scattering (CENNS)



where $\bar{\nu}$ is an antineutrino of any flavor (electron, muon, or tau) and X is a target nucleus. This is a reaction with no kinematic lower threshold. The coherence condition, i.e., where the nucleons recoil coherently rather than as an independent collection of objects, is $E_\nu \leq 30$ MeV for a range of target nuclei up to about $A = 82$ (lead target material). This is well met by reactor antineutrinos and, therefore, CENNS is a physically viable detection channel for CANs. The signal from an antineutrino-nucleus interaction in this channel is a very small nuclear recoil with maximum

energy determined by

$$T_{max} = \frac{E_\nu}{1 + \frac{M_N}{2E_\nu}} \quad (5)$$

where $M_N = (Z + N)u$ is the atomic weight of the target nuclei, Z denotes the number of protons in the target nuclei, and N is the number of neutrons in the target nuclei. The CENNS scattering cross section is (neglecting the small nuclear recoil energy term and the nuclear form factors, i.e., treating the nucleon distribution within the nucleus as spherically homogenous)

$$\frac{d\sigma}{dT}(E_\nu) = \frac{G_F^2}{4\pi} N^2 M_N \left(1 - \frac{M_N T}{2E_\nu^2} \right). \quad (6)$$

A good order of magnitude estimate is that this CENNS cross section is roughly 10^{-39} cm^2 , as compared to the IBD cross section that is roughly 10^{-42} cm^2 .

Although the CENNS reaction channel was theorized more than thirty years ago¹⁴ and is well-described by the standard model of particle physics it has not yet been observed in the laboratory. This is primarily because the recoil energies to be detected are very low and technology has not yet been developed or matured to the point where the low detector thresholds needed have been achieved. However, recent activity in the fundamental science community directed toward the observation of low energy dark matter¹⁵ and weakly interacting massive particles (WIMPs)¹⁶ is driving an R&D boom in low threshold detection technology. At the same time, academia has a long-standing interest in CENNS for detecting low energy solar neutrinos,¹⁷ low energy neutrinos from supernovae,¹⁸ for conducting searches for a postulated fourth neutrino,¹⁹ probing neutron distributions in nuclei,²⁰ as well as other more esoteric searches of new physics beyond the standard model.²¹ The convergence of these mutually supportive interests has engendered a number of suggested designs and renewed interest in building prototype CENNS devices. There have been a few proposals to monitor nuclear reactors using coherent antineutrino detectors.^{22,23,24,25} Very recently, Moroni et al.²⁶ pointed out that such a detector could be used for a first observation of CANs (although they do not comment on breeding blanket detection).

CENNS sensitivity to a breeding blanket

The purpose of the present study is to demonstrate that in principle a plutonium breeding blanket could be detected using an antineutrino detector that uses the CENNS detection channel to observe CANs from a breeding blanket. As such, where possible, the study assumed ideal conditions rather than specifying a design regarding the detector model. Due to the nature of the irreducible FAN background, the smallness of the neutron capture rate relative to the fission rate, and the inherently low detection rates for antineutrinos because of the weak interaction cross section, providing proof of principle is a nontrivial exercise.

Reactor model

The reactor model uses data regarding the isotopic composition, neutron fluxes, and one-group cross-sections taken from the model developed by Glaser et al.²⁷ This is a model of the Indian Prototype Fast Breeder Reactor (PFBR) that, like the Russian BN-600, is a liquid sodium cooled fast reactor that can be configured as a breeder. The reference model from 2007 uses a full three dimensional geometry and assumes fourteen burn up zones divided across 14 cells, with 6 cells representing the core, 4 the radial blanket, and 4 the axial blanket and with an inner core plutonium fraction of 21 percent and an outer core plutonium fraction of 28 percent. The calculation used a combination of the MCNP neutron transport code and ORIGEN2 depletion code following an iterative approach to model the core evolution and ran the core from start-up through to equilibrium with roughly six month refueling intervals, i.e., every 180 effective full power days (EFPDs). The estimated PFBR power output using this model was found to be 1.25 GWt with a net fissile material production rate of around 21 kg per year, at a breeding ratio of 1.057.

Input data was provided at nine different measurement points correlated with effective full power days ranging between 0 EFPDs at start of life and 540 EFPDs at core end of life. For the present study, the data at start of life was examined and the results are presented as this would be a crucial measurement point for a possible monitoring regime: assessing as early as possible (at start up or after refueling) whether or not a fast reactor was being run with a breeding blanket. The reactor model used is based on a reactor surrounded by a blanket, approximating the case without a blanket by simply subtracting the neutrino signal coming from the blanket. Values averaged over the first 90 EFPDs were used throughout the calculation. A cross check of the work showed that the results, in terms of sensitivity, do not change much later in the reactor cycle.

Therefore, strictly speaking, what was assumed here was not a comparison of a breeder reactor configuration versus a burner reactor configuration (where more fissile material is consumed than is produced). Rather a comparison was made between a “blanketed” breeder versus a “bare” breeder. This is not a precise simplification since a fast reactor operated without a blanket, i.e., as a pure burner, must be reconfigured by adding additional moderating rods and reflectors in order to compensate for the lack of a neutron sink provided by the blanket and thereby sustain the proper neutron balance and, hence, criticality. This is, however, a valid approximation since the prime difference between the two cases (with and without blanket) is in the core fission distribution and not in the fission rate (since the reactor is configured to operate at a steady power no matter the fuel distribution), nor in the core capture rate (since no uranium-238 is added in the moderating rods). Since the capture rate is the primary signal driver, there is no loss of applicability in making this assumption. Furthermore, no estimates have been provided as to how the PFBR would be configured as a pure burner, since this is not its intended design use, and any such model would be purely speculative.

To obtain the raw event rates from CENNS in various materials the reaction rates for both fission and neutron capture for the PFBR model were calculated using data on the one-group cross sections, isotopic mass content, and neutron fluxes per cell for each isotope according to the formula,

$$R_{i,j} = \phi_n^{i,j} \sigma_n^{i,j} N_A \frac{m_{i,j}}{m_{atomic}^i}, \quad (7)$$

where $R_{i,j}$ is the reaction rate for the i -th isotope in the j -th cell, $\phi_n^{i,j}$ is the fast neutron flux, $\sigma_n^{i,j}$ is the fast neutron one-group cross section for a given reaction, $m_{i,j}$ is the mass of isotope i present in cell j , m_{atomic}^i is the atomic weight, and N_A is Avogadro's number. Using the data from Glaser et al.²⁸ a total fission rate of 3.62×10^{19} fissions per second was obtained. Assuming a thermal energy of approximately 200 MeV per fission, this translates into 1.16 GWt in agreement with the reference model.

Neutrino yields per fission were obtained according to the prescription followed in Huber,²⁹ with a suitable extension to energies below 1.8 MeV based on a direct summation method using the fission yields for 400 keV incident neutron energy. With these neutrino yields, the following neutrino rates from the core are obtained: 1.7×10^{20} antineutrinos per second from fission (FAN) and 3.3×10^{19} from neutron capture (CAN). The same numbers for the blankets are: 1.40×10^{19} antineutrinos per second FAN and 3.4×10^{19} antineutrinos per second CAN. The energy distribution of the respective neutrino fluxes is shown in Figure 1.

Detector model

This study used a minimal source-detector “model” designed to capture all the relevant key physics. The detector was located at 25 m stand off from the core, an assumption designed to place the detector outside the reactor containment building

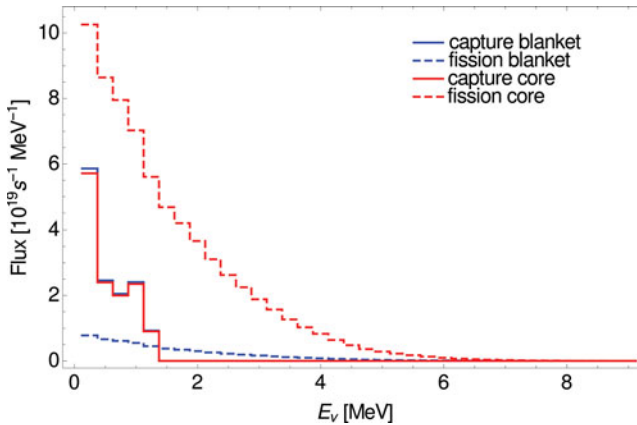


Figure 1. Contribution to the total antineutrino flux from various reactor regions. The solid (dashed) blue line indicates the antineutrino flux from blanket captures (fission). The solid (dashed) red line indicates the antineutrino flux from core captures (fission).

(a rectangular building 40 m wide, by 42 m long, by 55 m high³⁰) in a non-intrusive monitoring location. The detector was also assumed to be located on the surface. This is a more accessible emplacement than an underground site, especially at an existing reactor facility.

Moroni et al.'s paper³¹ demonstrates operation of a 52 gram prototype made of silicon with a recoil threshold of 30 eV. Deployed at sea-level, a background level of about 600 counts day⁻¹ kg⁻¹ keV⁻¹ was observed. A deployment of a prototype of this type of detector deep underground³² uncovered that much of this background is due to radioactivity in the shielding materials and, therefore, it is expected that this background may in fact be reducible by 1–2 orders of magnitude. Depending on the recoil energy cut this yields a predicted signal to noise ratio of 0.02–0.1. According to Moroni et al. about one-third of this background is from read-out noise and two-thirds are from actual particle interactions in the detector.

Scaling of this prototype into the 10s of kilogram range is, in principle, feasible and neither data rates nor power consumption are expected to become excessive. This study uses as a default assumption a signal to background ratio of 0.1, corresponding to 160 counts day⁻¹ kg⁻¹ keV⁻¹ for the silicon case with a flat distribution of backgrounds. For comparison, the TEXONO collaboration,³³ which uses reactor antineutrino-electron scattering to set an upper limit on the value of the neutrino magnetic moment, reports a background rate with moderate overburden (25 meters water equivalent) of about 1 to 10 counts day⁻¹ kg⁻¹ keV⁻¹ in a 1.06 kg germanium detector deployed 28 m from a 2.9 GWt reactor. The TEXONO detector, in terms of backgrounds from gamma radiation and fast neutrons, is very similar to the silicon charge-coupled devices (CCDs) used by Moroni et al. and this deployment nicely demonstrates that the reactor environment in itself does not lead to a large increase in backgrounds.

The CENNS signature is low-energy nuclear recoils, which result in a very high specific energy deposition per volume. For that reason, the most problematic backgrounds will be fast neutrons and alpha particles. Alpha particles can be reduced by careful selection of detector materials and shielding materials, whereas the fast neutron background is irreducible. Preliminary estimates indicate that the fast neutron induced background at the surface (from events such as cosmic ray muon induced spallation, ejection of a neutron from an atom due to the impact of a muon on the nucleus), in the region of interest corresponds³⁴ to 5 to 10 counts day⁻¹ kg⁻¹ keV⁻¹. Overall, this supports this work's assumption on backgrounds.

The reactor was treated as a point source in the calculation of the observed event rates. The reactor is an optically thin source, i.e., irrespective of the spatial distribution of antineutrino emission all emitting parts of the core can be “seen” by the detector. Therefore, the antineutrino production rate throughout the core can be treated as essentially homogenous and the active core size (core+blanket), 1.3 (1.6) meters in radius (height),³⁵ relative to the source-detector distance (25 meters) is small.

A perfect detection efficiency was assumed since no detector type was specified and the detector was assumed to be threshold-less in order to qualitatively assess what the threshold needed would be for detector materials of varying atomic mass A . The equations as presented in this paper were used for all physics calculations. To obtain the detector signal the following equation for the event rate $n(T)$ as a function of nuclear recoil energy T was used,

$$n(T) = \eta \int_0^\infty dE_\nu \phi_\nu(E_\nu) \frac{d\sigma}{dT}(E_\nu) \epsilon(E_\nu), \quad (8)$$

using for the normalization

$$\eta = \frac{1}{4\pi L^2} t n_{\text{targets}} \quad \text{with} \quad n_{\text{targets}} = \frac{N_A m_{\text{target}}}{N + Z}. \quad (9)$$

E_ν is the incident antineutrino energy in MeV, ϕ_ν is the neutrino flux in units of s^{-1} , $\frac{d\sigma}{dT}$ is the coherent scattering cross section from Eq. 6, and $\epsilon(E_\nu)$ is the efficiency of the detector. L is the distance between the reactor core and the antineutrino detector in meters. The data collection time is given by t in units of seconds. N_A is Avogadro's constant, m_{target} is the total mass of the target detector material in grams, N is the number of neutrons in the target nuclei, and Z denotes the number of protons in the target nuclei. Clearly, a real detector has a finite efficiency and all the results presented here would have to be scaled accordingly. A first generation detector like that discussed in Moroni et al. may have an efficiency of around 20 percent.

Statistical analysis

To determine the sensitivity of a CENNS detector, made of different possible target materials, to the presence of a breeding blanket a standard chi-squared test statistic was used

$$\chi^2 = \min_p \sum_i^{N_{\text{bins}}} \frac{(o_i - \bar{f}_i(p))^2}{o_i}, \quad (10)$$

where the number of observed events is given by $o_i := f_{co}^i + c_{co}^i + b^i$, f stands for events from fission (FAN), c for events from capture (CAN), b for background, and the subscript co denotes the contribution from the core. The i bins run over nuclear recoil energies. Variables without overbars are observed data, barred variables are the theoretical comparison. Here $\bar{f}_i := \bar{c}_{bl}^i + \bar{p}(f_{co}^i + \bar{c}_{co}^i) + \bar{b}^i$ with \bar{p} denoting the unknown reactor power, which is left free in the fit, and where the subscript bl denotes contributions from the blanket.

That is, the difference between \bar{f}_i and f_i is the term representing the antineutrino signal from captures in the blanket, c_{bl}^i , and its presence this χ^2 -function tests for. In principle, the fissions in the blanket f_{bl}^i contribute to the total reactor power and thus should also vary with \bar{p} in the fit, but in practice the sensitivity does not depend on this detail (since about 200 MeV are released per fission and only about

5 MeV per capture). For this simple analysis it is possible to neglect this dependence because the total contribution of fissions in the blanket to the reactor power is quite small and furthermore since these fissions produce a nearly identical spectrum of antineutrinos as do those from fissions in the core (at least at low energies), their inclusion would merely shift the value of \bar{p} at which the minimum χ^2 is found. The rate of capture antineutrino production does scale with reactor power, but we found in numerical tests that the overall sensitivity would be *higher* if we included this dependence. The reason is that in the current definition of f_i a smaller value \bar{p} can be used to obtain the same total rate as in f_i for any value of c_{bl}^i , whereas there is less freedom to make this relative adjustment when only the core contributions vary with power. Thus, this is a conservative approximation and in future work a detailed simulation of reactor with and without blanket at equal power needs to be performed. This χ^2 metric can be used to determine to what confidence level repeated measurement of the same parameter is expected to produce values within a given range. In this case, the parameter of interest is \bar{c}_{bl}^i the number of expected events for the i -th recoil energy bin. The presence of a blanket would be represented then by a preference for a non-zero value of \bar{c}_{bl}^i in the fit at a given confidence level.

As stated, the reactor power, which constrains the fission rates of the various antineutrino-producing isotopes, was left free in the fit. In principle, this somewhat reduces the sensitivity of the test metric to the value being fitted, i.e., the precision with which one can constrain the value of interest c_{bl}^i , through the loss of information. However, leaving the power free in the fit also reduces the overall dependence of the test on the power variable, i.e., leaving it as a free parameter allows a clean assessment of the detector's sensitivity to the signal without having it convoluted with the sensitivity of the test to other input variables. This choice amounts to assuming a deployment in which the coherent antineutrino detector is treated as a completely operator independent device, i.e., it is emplaced and little to no reactor power information is provided by the reactor operator to the inspecting party. In practice, precision power information is likely to be declared by the party being inspected (or could be obtained via a simultaneous measurement using a companion IBD antineutrino detector or more traditional thermal power monitoring methods). In that case, with the inclusion of power information the sensitivity of the chi-squared test to the presence of a breeding blanket increases.

A 90-day measurement time is assumed for all calculations, modeled after the 90-day IAEA safeguards goal to detect the timely diversion of irradiated direct use material, i.e., the estimated time it would take to convert material such as plutonium-239 in spent fuel into weapons use.³⁶ In this case the confidence with which the presence of a breeding blanket can be determined is given by the chi-squared $\Delta\chi^2$ metric

$$\Delta\chi^2(x) = \chi_i^2 - \chi_{min}^2 \quad (11)$$

where x is the variable of interest for the i -th recoil energy bin and χ_{min}^2 is the minimum value obtained, i.e., the best fit value for the observed data. For a one parameter fit $\Delta\chi^2 = 4$ represents the 95 percent confidence level.

Table 1. Calculated interaction rates for a 100 kg detector at 25 m standoff from the core after 90 days of data taking. T_{max}^c is the maximal nuclear recoil energy for scattering interactions with antineutrinos from fast neutron capture on uranium-238.

Material	Z	N	A	Core fission	Core capture	Blanket fission	Blanket capture	T_{max}^c [eV]
Deuterium	1	1	2	7943	183	733	188	1675
Helium	2	2	4	15886	367	1466	376	838
Silicon	14	14	28	111205	2569	10259	2634	120

Results

The calculated interaction rates for three possible target materials along with the maximum observable nuclear recoil energy are presented in Table 1, assuming 100 kilograms of detector material at 25 meter stand off and a measurement period of 90 days. The blanket FAN to CAN interaction rate ratio is about 4:1 representing a 25 percent level effect. The larger CENNS cross section, relative to IBD, has a nontrivial impact on detecting CANs at a rate that permits statistical sensitivity to the blanket. The emission rate of FAN to CAN is 3:1 and the fission to capture rate is roughly 2:1 for a fast reactor, so that the CAN interaction rate is at a 6:1 ratio relative to the FAN interaction rate.

There are two important facts to note about this detection channel: First, the observed event rate increases as the target material nuclear mass grows (the cross section is proportional to N^2 in Eq. 6). Second, the observed nuclear recoil energies decrease as the target material nuclear mass grows. The recoil energies are inversely proportional to M_N and the incident neutrino energies, on the order of a few MeV, are much smaller than the nuclear masses, on the order of a few GeV, so the M_N term dominates in Eq. 5. This sets up a tension and an optimization problem in detector design: the very low detector thresholds needed must be balanced with a reasonable event rate in order to detect the CAN signal. It is also possible to see that from Eq. 6 the only free parameter that can be controlled experimentally is the nuclear mass of the target material used in a CENNS detector. Therefore, the target material's atomic mass is a key parameter driving this detection channel, from the stand point of fundamental physics.

Figure 1 shows the contribution from FAN and CAN in the core and blanket to the total antineutrino flux of the reactor. As expected, the largest contribution to the total antineutrino flux comes from FAN produced in the core. A significant fraction of CANs are also produced in the core, however, the blanket CAN flux is higher than the core CAN flux. Note that at low energies the shape of the flux contributions differs significantly. The CAN antineutrino histogram has a much steeper slope than the FAN histogram, due to the strict 1.26 MeV upper limit on produced CANs. Figure 2 shows the resulting observed event rates for a small 10 kg silicon-28 detector. As a result of the shape difference in the flux contributions, the very low energy observed event rates are distinctly different for a blanketed core versus a bare core.

Lastly, Figure 3 shows the $\Delta\chi^2$ curves under various assumptions such as in the presence or absence of non-antineutrino backgrounds, for various detector

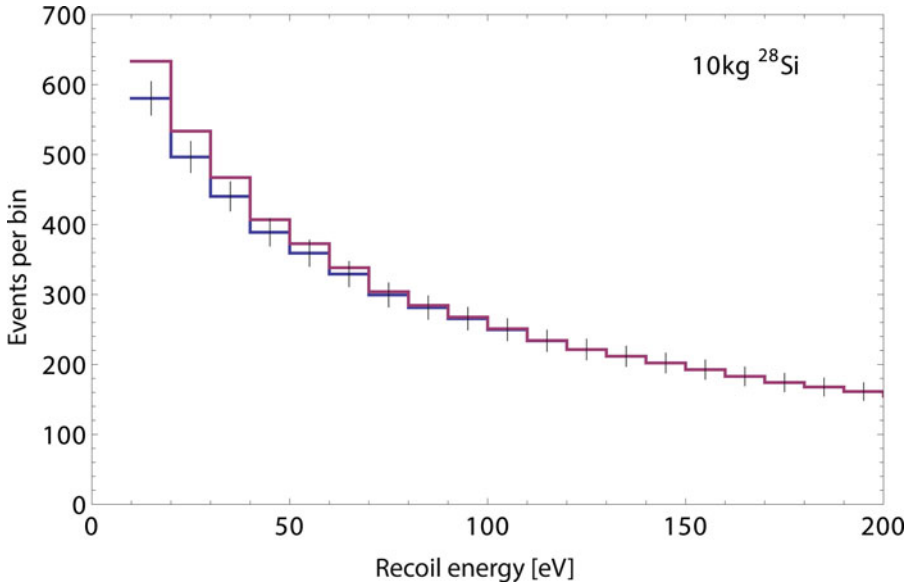


Figure 2. The detected nuclear recoil counts as a function of recoil energy for a 10 kg silicon-28 detector. The red line is for the core and the blanket combined; the blue line is for the core only. The black bars are statistical errors.

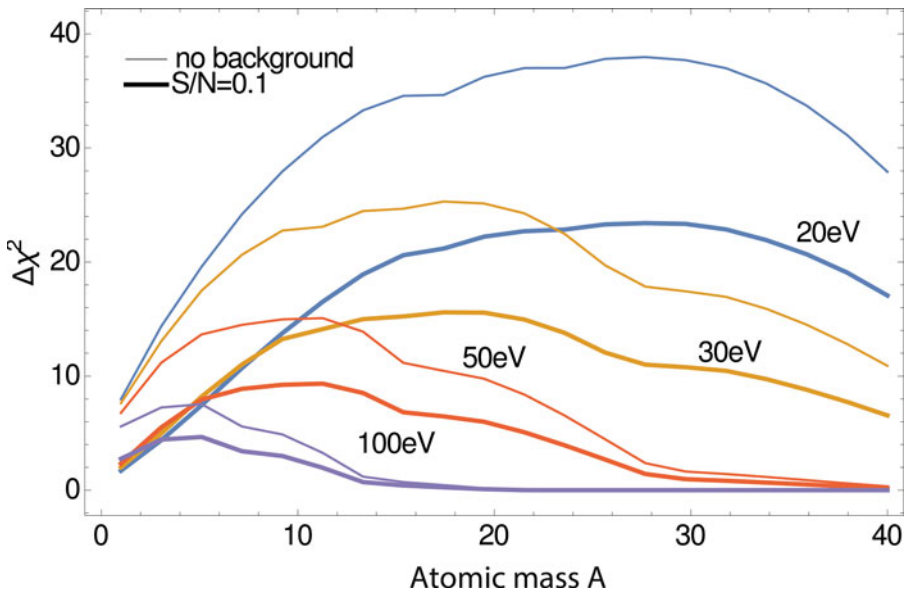


Figure 3. The χ^2 difference between a reactor with no blanket and one with a blanket as a function of the atomic mass A , where isoscalar targets were assumed, i.e., $A/2 = Z = N$. The reactor power is a free parameter in the fit. The detector mass is fixed at 100 kg and the data collection time is 90 days at a 25 m standoff. The colored lines are labeled by the detection threshold for the resulting nuclear recoils. Two cases are shown: neglecting backgrounds (thin lines) and including backgrounds with $S/N = 0.1$ (thick lines).

thresholds, and as a function of target material atomic mass. Figure 3 shows that the 95 percent confidence level ($\Delta\chi^2 = 4$) determination of the presence of a breeding blanket can be achieved across a range of target materials in the presence of backgrounds and across a range of detector thresholds.

Discussion

Now one can ask the question: what size detector is needed to achieve a 95 percent confidence level detection of a breeding blanket within 90 days at a 25 m standoff from a model PFBR? For example, note that natural silicon-28 has an isotopic abundance of 92.2 percent and that silicon-28 has 14 protons and 14 neutrons. Using these assumptions yields a required detector mass of approximately 36 kg of silicon-28 for a threshold of 30 eV. In Moroni et al.'s paper³⁷ the potential of a successor silicon-based CCD design to reach a threshold of 20 eV is discussed and, in this case, the required detector mass would go down to 17 kg.

It is clear that detection of the presence of a breeding blanket is feasible across a range of detector materials with low energy detection thresholds ranging between very stringent (20 eV) and low but less stringent (100 eV or more for nuclei below about $A = 9$). Note that 90 percent confidence level is considered high confidence within the intelligence community, in contrast to the 95 percent confidence level that was used here to assess sensitivity. Therefore, this analysis indicates that using a CENNS detector can provide credible information for possible monitoring or verification regimes regarding the presence or absence of a plutonium breeding blanket, while a fast breeder reactor is operating and without the need to access the containment vessel. Furthermore, this detector can be placed at some standoff outside the containment in building in a non-intrusive manner.

The tension between the low detector threshold and the desire for high event rates (to give a high confidence measurement in a reasonable time) is evident in Table 1. Therefore, detector design in a verification context will depend on optimizing between the time in which information is desired to detect anomalies and making quantitative assertions with higher confidence. The ability to detect the presence of breeding blanket CANs against the core FAN background is driven by reasonably large event rates as well as the shape difference in the antineutrino flux at low energies between the FAN and CAN contributions to the total event rate. The nuclear recoil energy is proportional to the square of the incident antineutrino energy (see Eq. 5). This means that the detection focus must be on the lower energy events, as opposed to those near the maximum recoil limit, in order to obtain meaningful information. In other words, developing this technology for safeguards purposes should focus on capturing as much of the low energy spectrum as possible, not just on obtaining high event rates near threshold.

The signal strongly increases with decreasing energy, whereas, the background stays flat. Therefore, the S/N ratio will improve for lower detection thresholds, or at fixed threshold for a lower atomic mass A of the target. However, the total number of events will decrease with a smaller atomic mass and, hence, for a given threshold

a certain optimum atomic mass exists, see [Figure 3](#). Note that a flat background, while being a reasonable assumption, may not be the case in a real detector and the optimization question has to be investigated for the actually found backgrounds.

Lastly, it should be pointed out that the distance between the core and detector will affect the measurement time and the detector volume. The neutrino flux is isotropic and so follows a simple $1/L^2$ drop off at a distance L from the core. In principle, the detector could be located farther away provided a larger (more expensive) detector was built to maintain the 90-day measurement time. Alternatively, a shorter measurement time could be attained by locating the same sized detector closer to the core or by building a detector with a larger target mass. Deployments closer than 10 meters are unlikely due to the typical design of a reactor core which involves the core size itself, extensive shielding, cooling and other operational equipment.

Conclusion

The present study finds that coherent elastic neutrino-nucleus scattering antineutrino detectors are a viable and nonintrusive technology that could be used to monitor a plutonium breeding blanket at liquid sodium-cooled fast breeder reactors. Our preliminary analysis shows that it would be possible to determine the presence of a breeding blanket at a reactor such as the Indian Prototype Fast Breeder Reactor within 90 days using less than 100 kg of detector located at 25 m standoff from the reactor core, assuming a 100 percent detection efficiency. Such a detector would have to have a nuclear recoil energy threshold of less than 100 eV. A silicon-based detector has observed backgrounds matching the levels assumed in this study, been demonstrated to be feasible at sea-level deployment, i.e., above ground, and could therefore be located just outside a reactor containment building allowing non-intrusive monitoring of the core.

In combination with data from an incoherent inverse beta decay antineutrino detector, which can constrain the reactor power and be used to estimate the core plutonium content, it may prove possible for CENNS detector data to be used to help estimate the plutonium content in the breeding blanket itself. Determining the extent of this sensitivity and the optimal combination of IBD and CENNS detectors to get the most from the antineutrino rate and shape data, especially in the presence of more precise backgrounds and with greater detector specificity, would be a useful area of further research. This would give a well-rounded assessment of the qualitative (presence or absence of the blanket in the core vessel) and quantitative (plutonium amount and grade in the blanket) estimates of value for verification or safeguards efforts that could be made using coherent antineutrino detectors.

Acknowledgements

The authors are indebted to: A. Glaser for sharing data from his model of the Indian PFBR; J. Formaggio for discussion about CENNS detectors; F. von Hippel, Z. Mian, M. V. Ramana, and T. Shea for comments on early drafts of this work.

Funding

The work of B.K.C was supported by the John D. & Catherine T. MacArthur Foundation, “Support for Education and Training of the Next Generation of Nuclear Non-Proliferation, Arms Control, and Disarmament Scientists.” The work of P.H. was in part supported by the U.S. Department of Energy under contract DE-SC0013632.

Notes and references

1. 2000 Plutonium Management and Disposition Agreement as amended by the 2010 Protocol, “Agreement between the Government of the United States and the Government of the Russian Federation Concerning the Management and Disposition of Plutonium Designated as No Longer Required for Defense Purposes and Related Cooperation” (2010).
2. A. M. Judd, *An Introduction to the Engineering of Fast Nuclear Reactors*, (New York: Cambridge University Press, 2014).
3. C. Bemporad, G. Gratta, and P. Vogel, “Reactor-Based Neutrino Oscillation Experiments,” *Reviews of Modern Physics* 74 (2002): 297–328.
4. L. A. Mikaelyan, *Proceedings of the International Conference on Neutrino Physics*, vol. 2 (1977, unpublished): 383–387.
5. V. A. Korovkin, S. A. Kodanev, A. D. Yarichin, A. A. Borovoi, V. I. Kopeikin, L. A. Mikaelyan, and V. D. Sidorenko, “Measurement of Burnup of Nuclear Fuel in a Reactor by Neutrino Emission,” *Atomic Energy* 56 (1984): 233–239.
6. Y. V. Klimov, V. I. Kopeikin, L. A. Mikaelyan, K. V. Ozerov, and V. V. Sinev, “Neutrino Method of Remote Measurement of Reactor Power and Power Output,” *Atomic Energy* 76 (1994): 123–127.
7. A. Bernstein, N. S. Bowden, A. Misner, and T. Palmer, “Monitoring the Thermal Power of Nuclear Reactors with a Prototype Cubic Meter Antineutrino Detector,” *Journal of Applied Physics* 103 (2008): 074905 (10 pages); N. S. Bowden, A. Bernstein, S. Dazeley, R. Svoboda, A. Misner, and T. Palmer, “Observation of the Isotopic Evolution of Pressurized Water Reactor Fuel Using an Antineutrino Detector,” *Journal of Applied Physics* 105 (2009): 064902 (8 pages).
8. G. Boireau et al. (Nucifer Collaboration), “Online Monitoring of the Osiris Reactor with the Nucifer Neutrino Detector,” arXiv:1509.05610 [physics.ins-det] (2015).
9. A. Bernstein, G. Baldwin, B. Boyer, M. Goodman, J. Learned, J. Lund, D. Reyna, and R. Svoboda, “Nuclear Security Applications of Antineutrino Detectors: Current Capabilities and Future Prospects,” *Science and Global Security* 18 (2010): 127–192.
10. A. C. Hayes, H. R. Trellue, M. M. Nieto, and W. B. Wilson, “Antineutrino Monitoring of Burning Mixed Oxide Plutonium Fuels,” *Physical Review C* 85 (2012): 024617 (3 pages).
11. C. Copeland, “Monitoring Under the Plutonium Management and Disposition Agreement: The Prospects of Antineutrino Detection as an IAEA Verification Metric for the Disposition of Weapons-Grade Plutonium in the United States,” (M.S. thesis, Massachusetts Institute of Technology, 2012).
12. E. Christensen, P. Huber, P. Jaffke, and T. Shea, “Antineutrino Monitoring for Heavy Water Reactors,” *Physical Review Letters* 113 (2014): 042503 (5 pages).
13. E. Christensen, P. Huber, and P. Jaffke, “Antineutrino Reactor Safeguards: A Case Study of the DPRK 1994 Nuclear Crisis,” *Science and Global Security* 23 (2015): 20–47.
14. D. Z. Freedman, “Coherent Effects of a Weak Neutral Current,” *Physical Review D* 9 (1974): 1389–1392; A. Drukier, and L. Stodolosky, “Principles and Applications of a Neutral-Current Detector for Neutrino Physics and Astronomy,” *Physical Review D* 30 (1984): 2295–2309.

15. R. Bernabei et al. (DAMA Collaboration), “New Results from DAMA/LIBRA,” *European Physical Journal C* 67 (2010): 39–49; C. E. Aalseth et al. (CoGeNT Collaboration), “CoGeNT: A Search for Low-Mass Dark Matter Using p -Type Point Contact Germanium Detectors,” *Physical Review D* 88 (2013): 012002 (20 pages); R. Agnese et al. (CDMS Collaboration), “Silicon Detector Dark Matter Results from the Final Exposure of CDMS II,” *Physical Review Letters* 111 (2013): 251301 (6 pages).
16. R. Agnese et al. (SuperCDMS Collaboration), “Search for Low-Mass Weakly Interacting Massive Particles with SuperCDMS,” *Physical Review Letters* 112 (2014): 241302 (6 pages); G. Angloher et al. (CRESST Collaboration), “Results on Low Mass WIMPs Using an Upgraded CRESST-II Detector,” *European Physical Journal C* 74 (2014): 3184 (6 pages).
17. J. Billard, L. E. Strigari, and E. Figueroa-Feliciano, “Solar Neutrino Physics with Low-Threshold Dark Matter Detectors,” *Physical Review D* 91 (2015): 095023 (13 pages).
18. C. J. Horowitz, K. J. Coakley, and D. N. McKinsey, “Supernova Observation via Neutrino-Nucleus Elastic Scattering in the CLEAN Detector,” *Physical Review D* 68 (2003): 023005 (7 pages).
19. A. J. Anderson, J. M. Conrad, E. Figueroa-Feliciano, C. Ignarra, G. Karagiorgi, K. Scholberg, M. H. Shaevitz, and J. Spitz, “Measuring Active-to-Sterile Neutrino Oscillations with Neutral Current Coherent Neutrino-Nucleus Scattering,” *Physical Review D* 86 (2012): 013004 (11 pages).
20. K. Patton, J. Engel, G. C. McLaughlin, and N. Schunck, “Neutrino-Nucleus Coherent Scattering as a Probe of Neutron Density Distributions,” *Physical Review C* 86 (2012): 024612 (9 pages).
21. K. Scholberg, “Prospects for Measuring Coherent Neutrino-Nucleus Elastic Scattering at a Stopped-Pion Neutrino Source,” *Physical Review D* 73 (2006): 033005 (9 pages).
22. C. Hagmann and A. Bernstein, “Two-Phase Emission Detector for Measuring Coherent Neutrino-Nucleus Scattering,” *IEEE Transactions on Nuclear Science* 51 (2004): 2151–2155.
23. U. S. Department of Energy, Pacific Northwest National Laboratory, J. L. Orrell and J. I. Collar, “Final Report for Monitoring of Reactor Antineutrinos with Compact Germanium Detectors,” PNNL-18592, July 2009.
24. D. Yu. Akimov et al. (RED Collaboration), “Prospects for Observation of Neutrino-Nuclear Neutral Current Coherent Scattering with Two-Phase Xenon Emission Detector,” *Journal of Instrumentation* 8 (2013): P10023 (11 pages).
25. G. Fernandez Moroni, J. Estrada, G. Cancelo, E. Paolini, J. Tiffenberg, C. Bonifazi, J. Molina, and J. Moro, “New Instrument for Neutrino Detection: Coherent Neutrino-Nucleus Interaction Experiment (CONNIE),” (talk presented at the 33rd International Cosmic Ray Conference, Rio de Janeiro, Brazil, 2013).
26. G. Fernandez Moroni, J. Estrada, E. E. Paolini, G. Cancelo, J. Tiffenberg, and J. Molina, “Charge Coupled Devices for Detection of Coherent Neutrino-Nucleus Scattering,” *Physical Review D* 91 (2015): 072001 (9 pages).
27. A. Glaser and M. V. Ramana, “Weapon-Grade Plutonium Production Potential in the Indian Prototype Fast Breeder Reactor,” *Science and Global Security* 15 (2007): 85–105.
28. Glaser, “Plutonium Production in the Prototype Fast Breeder Reactor.”
29. P. Huber, “Determination of Antineutrino Spectra from Nuclear Reactors,” *Physical Review C* 84 (2011): 024617 (16 pages).
30. Indira Gandhi Centre for Atomic Research (IGCAR), *Prototype Fast Breeder Reactor: Preliminary Safety Analysis Report*, February 2004, Table 1.2, sub-item 9.
31. Moroni, “Charge Coupled Devices for Neutrino-Nucleus Scattering,” 4–7.
32. A. E. Chavarria et al. (DAMIC Collaboration), “DAMIC at SNOLAB,” arXiv:1407.0347 [physics.ins-det] (2014).

33. H. T. Wong et al. (TEXONO Collaboration), “Search of Neutrino Magnetic Moments with a High-Purity Germanium Detector at the Kuo-Sheng Nuclear Power Station,” *Physical Review D* 75 (2007): 012001 (16 pages).
34. The total number of fast neutrons passing through a 10 kg silicon detector is of the order of 10^7 in a 90 day period. However, less than 0.5 percent produce recoils in the CENNS window and an even smaller fraction ends up in the CAN blanket signal region.
35. Glaser, “Plutonium Production in the Prototype Fast Breeder Reactor,” 87.
36. National Nuclear Security Agency, Los Alamos National Laboratory, P. Pan, B. Boyer, and C. Murphy, “Guidance for Research Reactors and Critical Assemblies,” LA-UR-12-26349, September 2012, 9.
37. Moroni, “Charge Coupled Devices for Neutrino-Nucleus Scattering,” 7–8.